Voxel Based Analysis of Tissue Volume MRI Data

N. A. Thacker, D. C. Williamson, M. Pokric

20th July 2003

Abstract

This document has been written to illustrate the role that assumptions play in the design of image analysis algorithms. We present several common methods for the segmentation of MR data on the basis of underlying tissue. These methods, which may appear disparate at first sight, are discussed and related in terms of the assumptions regarding the data fornmation process needed to derive them. We summarise the use of these techniques using a flow diagram which makes explicit the questions which need to be addressed in order that they are used appropriately.

Introduction

When attempting to segment data in an image, though we may be unaware of it, we are really asking a question which has no perfect answer. In common with many other data analysis tasks the best thing that we can determine is only the probability of a particular interpretation. It is a simple fact that in order for a program to segment a data set well it must use statistical principles.

Many segmentation methods work by applying calculations which at first sight appear to have nothing in common with either probability theory or statistics, but if we wish to explain the best approaches to MR image segmentation we must be able to relate these techniques to the statistical models that they are based upon. The most direct piece of information which we can obtain from data is in the form of a conditional probability. $P(C|D)$ is the probability of the interpretation C given the data D. Given such probabilities for each pixel in an image we can segment regions or locate the boundaries between tissues. If the method (or algorithm) used to determine these probabilities is appropriate, then the regions and boundaries determined in this manner will be optimal. That is, they will (by definition) have extracted all of the useful information relating to the problem from the data. Determining that an algorithm is appropriate amounts to being able to confirm that the assumptions underlying the statistical approach are valid. To do this we must first know what these assumptions are. Areas of algorithmic research which give rise to image processing algorithms are fundamentally linked to matching assumptions to data sets. Though it is possible to develop good algorithms blindly (by guesswork and testing) it is always better to apply a statistical methodology, systematically testing the effects of any assumption on the result.

The consequence of all of this is that there is no technique that can be guaranteed to work on any data set, that is a “magic bullet". For any method to work it must be applied to data which falls within the range of behaviour for which it has been designed. Different algorithms have varying ranges of applicability. Algorithms which make the most assumptions regarding the data often have very limited use in comparison to those which take into account a broader range of data characteristics. Though algorithms which make a large number of assumptions can often be simple it is not necessarily true that complex algorithms will always perform better. The extra complexity must be used wisely and for good reason. Extra complexity can just as easily result in unreliability as in improved results. These are the issues that algorithm designers consider when developing a new technique.

The following sections explain the various approaches to tissue segmentation algorithms which deliver either boundaries or labelled regions. We start with the simplest and the assumptions upon which they are based and work gradually towards a more general solution for use on a broad range of data. Technical information is given in detail in maths boxes for those who are mathematically literate.

Simple Image Segmentation.

The first thing we need to know about MR data is that to a very good approximation the greylevel values in an image can be assumed to be formed by a linear process. This means that the contribution to the signal in any pixels is simply proportional to the relative fractions of each tissue within the voxel [4] (see Box 1). Typical images (acquired using a 1.5 Tesla Phillips scanner) are shown in figure 1.

Armed with this assumption it is possible to justify simple approaches to tissue boundary identification, such as thresholding, where a label asignment is made according to each grey level being above or below a specified grey level value. This is because a given greylevel corresponds directly to particular fractional proportions of a given pair of tissues. A fraction of 50 percent of two tissues defines the most likely location for a boundary. This is used as the basis for many visualisation techniques which require the identification of surfaces (eg: "marching cubes" [5]).

The expression for the signal intensities of pure tissues in an inversion recovery spin-echo (IRSE) sequence follows directly from the Bloch equations and is

$$S = N(H)(1 - 2e^{(-TI/T_1)} + 2e^{(-(TR-\tau)/T_1)} - e^{(-TR/T_1)})e^{(-TE/T_2)}$$

where $N(H)$ is the spin density and TE is the echo time. The modern equivalent to (IRSE) is the inversion recovery turbo spin-echo (IRTSE) sequence. The expression for the signal intensities for pure tissues is

$$S = N(H)(1 - 2e^{(-TI/T_1)} + 2e^{(-(TR-T_sN_f)/T_1)} - e^{(-TR/T_1)})e^{(-TE_{eff}/T_2)}$$

where T_s is echo spacing and N_f is the factor number of the TSE train.
The linear dependency of expressions on $N(H)$ are typical for MR sequences with the consequence that the grey level within any voxel g_v can be written as the linear contribution from a set of partial volumes

$$g_v = p_1G_1 + p_2G_2 + p_3G_3 + ... + p_NG_N$$

with

$$p_1 + p_2 + p_3 + ... + p_N = 1$$

where p_n is the nth partial volume and G_n the mean grey level for pure tissue.

Box 1: Image Formation in MR.

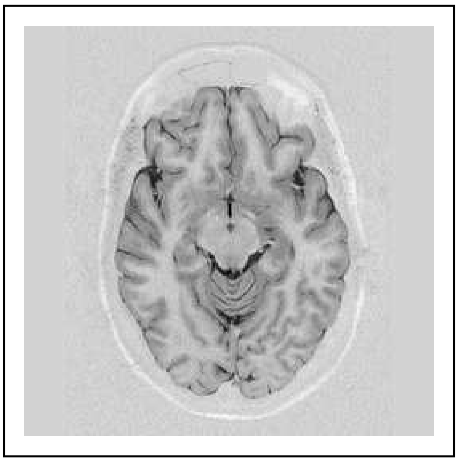

(a) Inversion Recovery Turbo Spin Echo

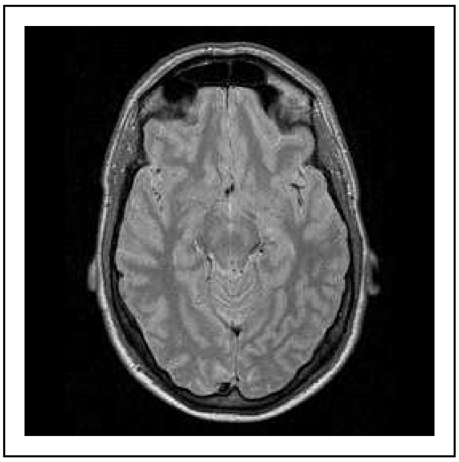

(b) Variable Echo (Proton Density)

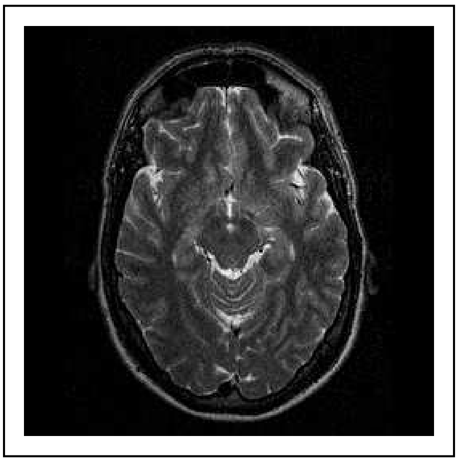

(c) Variable Echo (T2)

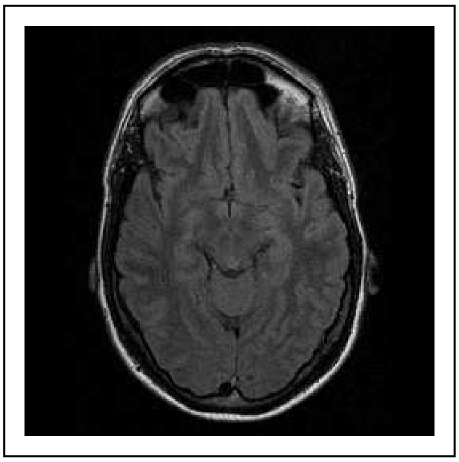

(d) FLAIR

Figure 1: Image Sequences

Such an algorithm will deal adequately with identification of tissue boundaries provided that we are always looking for the boundary between the same two tissues and that there are no processes during image formation which invalidate our assumption. Unfortunately, both of these requirements are generally not met by the majority of images.

The most likely failiure in the assumptions behind the thresholding approach is that the data is not simply composed of two tissues. Figure 2 (a) illustrates the use of a thresholding process on the data in Figure 1(b). In this case an attempt has been made to identify only grey matter voxels. As can be seen, other areas are also identified around the outside of the head using this process.

A technique for boundary location which can work with multiple tissues is based closely on the way that humans percieve image data. The idea involves identifying the boundaries between otherwise homogenous regions by locating the positions of maximum contrast or "edges". Edge detectors are more common in the field of machine vision than medical image analysis [6] and are generally based on the idea of computing the local spatial derivative of an image after smoothing. Taking the peak of this derivative defines the maximum transition point between the tisues which is generally also the 50 percent probability boundary between any two adjacent tissues (see Box 2). Complete extraction of such boundaries would enable unambiguous labelling of regions.

Detection of edge boundaries in 2D is generally performed in a manner similar to the following;

- Convolution of the image with a spatial noise reduction filter, (eg: a Gaussian) $I' = I \otimes G(x, y)$.
- Calculation of local image gradients $\delta_x = (\partial I/\partial x)$ (ie: $I' \otimes (-1, 0, 1)$) , $\delta_y = (\partial I/\partial y)$ (ie: $I' \otimes (-1, 0, 1)^T$).
- Calculation of an edge strength $E(x, y) = \delta_x^2 + \delta_y^2$
- Identification of edges as those voxels with edge strengths above a statistical threshold ($E(x, y) > k$) and less than no more than two of its neighbours (implying simple linear connectivity).

Box 2: A simple edge detector.

While this technique will work well on sharp boundaries the more slowly varying partial volume regions which occur in MR data can cause problems with such an approach. This issue is a particular problem for thick slices where as many as 40% of voxels may be affected [16]. Typical results for an edge detector are shown in Figure 2 (b), it is clear that not all tissue boundaries have been located, in particular those between the grey and white matter regions. This is because edge detectors are in effect a hypothesis test process and the ability to identify edges is a function of the local contrast to noise characteristics. In the brain in particular the partial volume process reduces contrast to noise for any boundary which is not close to perpendicular to the plane of acquisition.

Accounting for the partial volume behaviour of multiple tissues can be compensated for but overcoming contrast to noise limitations may require more information than is present in a single image. Techniques have been devevoped for use with specific pairs of image sequences ([18]). In fact the general solution for the proportion of each of N tissues within a voxel is an exercise in linear algebra and requires N-1 images (see Box 3).

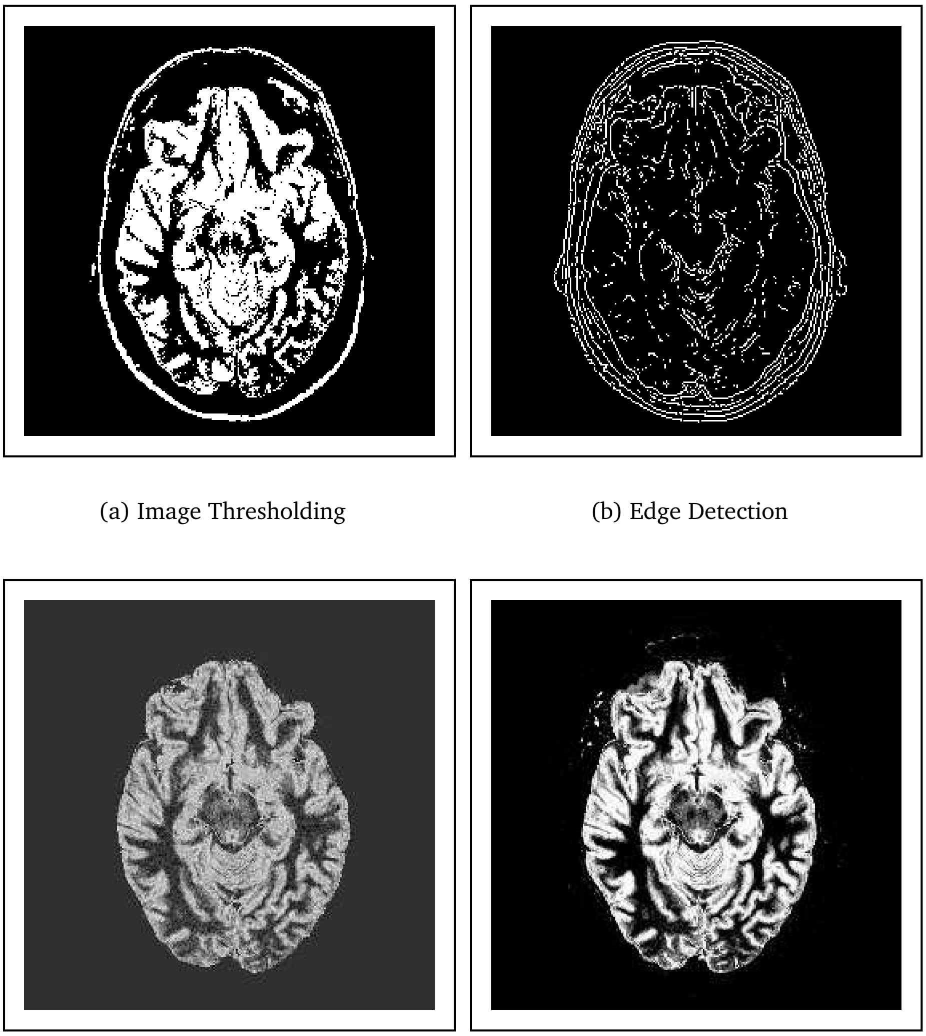

(a) Image Thresholding

(b) Edge Detection

(c) Solution of Linear Equations

(d) Probable Volume Estimate

Figure 2: Image Segmentation

The three linear equations for the grey level value in two images and the total proportion constraint can be solved for each tissue of three tissues (eg: c,w,g) within each voxel v as follows:

$$p_{cv} \;=\; \frac{g_{1v}(G_{2w} - G_{2g}) \;-\; g_{2v}(G_{1w} - G_{1g}) \;-\; (G_{1g}G_{2w} - G_{2g}G_{1w})}{(G_{1c} - G_{1g})(G_{2w} - G_{2g}) - (G_{2c} - G_{2g})(G_{1w} - G_{1g})}$$

$$p_{gv} \;=\; \frac{g_{1v}(G_{2c} - G_{2w}) \;-\; g_{2v}(G_{1c} - G_{1w}) \;-\; (G_{1w}G_{2c} - G_{2w}G_{1c})}{(G_{1g} - G_{1w})(G_{2c} - G_{2w}) - (G_{2g} - G_{2w})(G_{1c} - G_{1w})}$$

and

$$p_{wv} \;=\; 1 \;-\; p_{cv} \;-\; p_{gv}$$

Box 3: Direct estimation of partial volume fractions using linear algebra.

Such an approach will deliver unbiased estimates of tissue proportion ([9]). Typical results using a three tissue model and the first pair of images shown in Figure 1 are shown in Figure 2 (c). Notice that the data has been skull stripped, as the method can only deliver correct estimates for the tissues within the model (in this case grey matter, white matter and cranial fluid), meaning it cannot deal with unexpected behaviour. From a medical standpoint this is equivalent to saying that it can only deal with normal tissues. Further, the assumption of a pure linear model is equivalent to the statistical assumption of noise free data. The consequence of this is that estimates of tissue proportion are noisy (with a typical random uniform Gaussian noise level of 15 %) and values can be outside the physical range of 0-100 percent. Dealing with both of these problems requires a more overtly statistical approach to data analysis.

What we must do is apply the methodology of probability theory directly to the modelling of data. This involves constructing a likelihood model for each tissue component present in the data. A common approach (available in most image analysis software packages) involves modelling only the pure tissue distributions and generates probailities which correspond to the most likely tissue label given the data. However, in order to account for partial volume effects partial volume distributions must also be modelled. Modelling of partial volumes using additional Gaussian terms turns out to be both inappropriate and unstable [13]. In addition, in order to model the image formation process it turns out that we can no longer compute probabilities of tissue labels, we must compute probabilities of partial volume fractions [15]. This is a subtle shift which may be seen to be at odds with the approach taken by the majority of papers in this area. It is however, entirely consistent with our earlier observations regarding segmentation on the basis of tissue volume and necessary if partial volume effects are to be correctly dealt with.

The various parameters in the density model must be determined using an optimisation algorithm to minimise the difference between the model and the data. The simplex algorithm [7] and Expectation Maximisation [8] are commonly used for this purpose. Estimation of relative volumetric tissue proportions can then be made by the direct use of Bayes theory (see Box 4).

The total probability of getting a particular set of grey level values (g) within a region of the image comprised of three tissues (1-3) and two sets of partial volumes (12, 21 and 23 , 32) (eg: Figure 3) can be written as;

$$P_{tot}(g) \ = \ f_a P_1(g) \ + \ f_b P_2(g) \ + \ f_c P_3(g) \ + \ f_d P_{12}(g) \ + \ f_d P_{21}(g) \ + \ f_e P_{23}(g) \ + \ f_e P_{32}(g)$$

Were the set of f parameters are adjusted to match the sample of data. The separate components for the likelihood of each grey level value from each tissues can be written as;

$$P(g|1) \ = \ f_a P_1(g) \ + \ f_d P_{12}(g)$$

$$P(g|2) \ = \ f_b P_2(g) \ + \ f_d P_{21}(g) \ + \ f_e P_{23}(g)$$

$$P(g|3) \ = \ f_c P_3(g) \ + \ f_e P_{32}(g)$$

We can now use Bayes theory to compute the conditional probability of a tissue given a grey level value as;

$$P(n|g) \ = \ P(g|n)/P_{tot}(g)$$

However, inclusion of the partial volume terms as shown here means that $P(n|g)$ is no longer simply the probability of the label of the voxel. It is now an estimate of the mean volumetric contribution to the formation of a voxel with grey level g.

Box 4: Bayes classification of grey level vaues for three tissues.

The delivered probabilities are exactly those described in the introduction. If the derived frequency model is an accurate representation of the data then the result delivered by this technique is the most probable tissue volume fraction within each voxel for data comprised of tissues with the same prior proportions. This is the optimal solution to the problem of segmenting data on the basis of voxel grey levels in terms of a minimal error on the volume estimates. The technique will give accurate estimates with multiple tissues (N) on a single image provided that the grey level distributions do not overlap significantly, in contrast to the previous solution of linear equations approach which always requires $N-1$ images. Further, overlapping tissues can be eliminated by the use of multiple images, as ambigious regions in the data can be separated with additional independant information. However, this does involve a slightly more complicated analysis in order to determine all of the parameters in the multi-dimensional model. Extension of this technique to deal with pathological (unmodelled) tissues can be incorporated by allowing an additional category for infrequently occuring data [10] (see Box 5). Typical results from this technique, working now with all four images shown in Figure 1, are shown in Figure 2 (d). The model used now includes six separate tissue terms, including fat, muscle and air/bone, as well as the usual three brain tissues. Notice that in comparison to Figure 2(c) (the linear solution approach), we do not need skull stripping in order to get a reasonably unambiguous segmentation, though a few errors are made around the margins of the head due to residual ambiguitiy in the 4d data space.

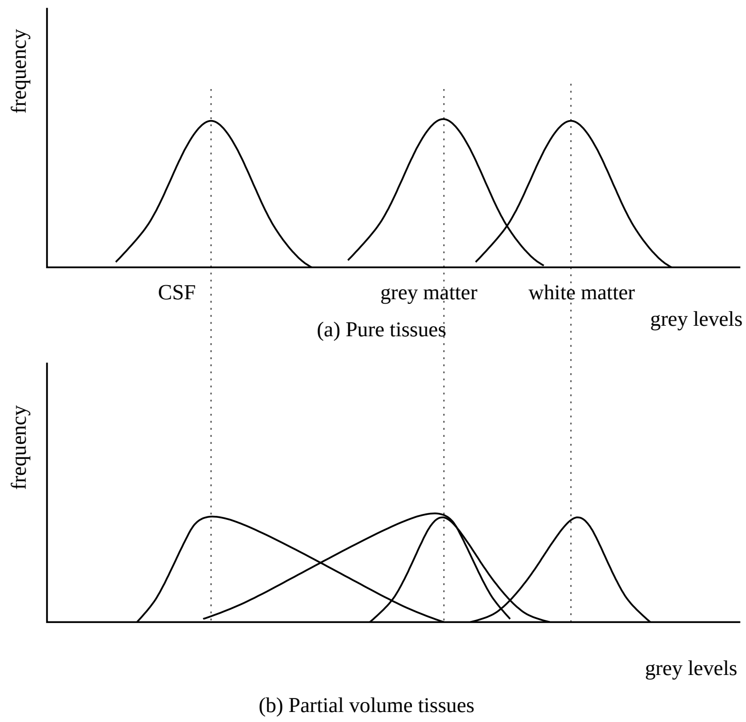

Figure 3: Probability distributions for brain tissues. *Pure tissues have Gaussian distributions and partial volume distributions for paired tissue combinations take the form of a triangular distribution convolved with a Gaussian which is intended to model the response function of the measurement system.*

For multi-spectral data $\mathbf{g}$ we must define a multi-variate distribution for each pure tissue t.

$$P_t(\mathbf{g}) \ = \ \alpha_t e^{-(\mathbf{g}-\mathbf{G_t})^T C_t (\mathbf{g}-\mathbf{G_t})}$$

Where G_t is the mean tissue vector and C_t its covariance and α chosen to give unit normalisation. Partial volume distributions can be modelled along the line between two pure tissue means G_t G_s.

$$P_{ts}(\mathbf{g}) \ = \ \beta_{ts} P_{ts}(h) e^{-(\mathbf{g}-\mathbf{h}.\mathbf{g}/|h|)^T C_h (\mathbf{g}-\mathbf{h}.\mathbf{g}/|h|)}$$

with $\mathbf{h} \ = \ (\mathbf{g}-\mathbf{G_s})C_h(\mathbf{G_t}-\mathbf{G_s})/|(\mathbf{G_t}-\mathbf{G_s})C_h(\mathbf{G_t}-\mathbf{G_s})|$, $C_h \ = \ C_t\mathbf{h} \ + \ C_s(1-\mathbf{h})$ and $P_{ts}(h)$ is the 1D partial volume distribution such as used in Figure 3. Parameters for the model can be iteratively estimated by taking weighted averages over the selected volume V using a process generally referred to as Expectation Maximisation (EM).

$$f_t \ = \ \sum_v^V P(t|\mathbf{g_v}) \quad , \quad f_{ts} \ = \ f_{st} \ = \ \frac{1}{2}\sum_v^V P(ts|\mathbf{g_v}) \ + \ P(st|\mathbf{g_v})$$

$$G'_t = \frac{1}{V}\sum_v^V P(t|\mathbf{g}_v)\mathbf{g}_v \quad , \quad {C'}_t^{-1} \ = \ \frac{1}{V}\sum_v^V P(t|\mathbf{g}_v)(\mathbf{g}_v - \mathbf{G_t}) \otimes (\mathbf{g}_v - \mathbf{G_t})^T$$

Unknown tissues are included in the Bayesian formulation by including a fixed extra term f_o for outlying data points in $P_{tot}(\mathbf{g})$.

Box 5: Multispectral modelling with an unknown tissue.

Bayesian approaches can be extended to make use of prior knowledge regarding expected spatial location or local correlations between structures. This can be simply incorporated by including additional prior probability terms and can result in further improvements in the appearance of segmentation. The approach of modelling spatial distributions using Markov random fields is quite popular. However, the common use of Gibbs distributions is an inapropriate use of methodology from theoretical physics. The correct approach, based upon quantitative use of probaility theory, is described in [14]. This method involves predicting the most likely interpretation of a central voxel given its neighbours based upon a statistical example of sample data. An approximation suitable for MR segmentation, based upon charaterising local structure using grey level slope is described in [20]. This approach can be thought of as combining the information available to edge based segmentation approaches with that available in the raw grey levels. Figure 4 (a) shows an axial slice of a human leg, three tissues are readlily visible. The darkest is cortical bone, thintermediate is muscle and the brightest is fat. Analysis of this image using a partial volume analysis results in a muscle segmentation image shown in Figure 4 (b). Results obtained when including a edge strenght model are shown in Figure 4 (c). Voxels which could not be correctly analysed previously based soley upon grey-level value can now be unambiguosly attributed to the correct tissue components. Similar results are also obtained for brain images in which partial volumes from bone and fat can produce grey-levels which are consistent with grey matter [20].

The common technique of introducing additional prior terms (particularly for exaple the use of a ”normal atlas”) produces biases to any quantitative measurement and great care needs to be taken in order to use results from any Bayesian measurement in quantitative tasks [12]. A more complete description of this and other problems with the practical use of Bayesian approaches is covered in [2].

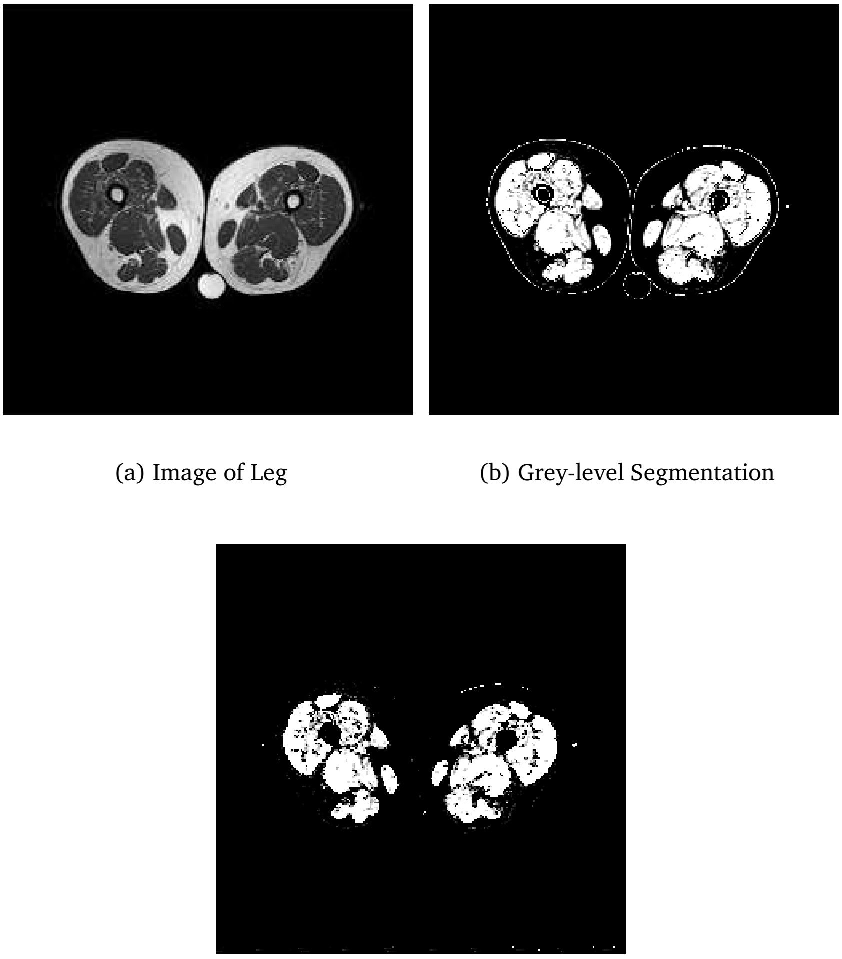

(a) Image of Leg

(b) Grey-level Segmentation

(c) Grey-level/slope Analysis

Figure 4: Combining Edge and Grey Level Information

Dealing with Data In-Homogenaeity

Having dealt with the issues of partial volumes, noise and pathological data the only remaining problem which is likely to be encountered in real data is that the assumption of a pure linear model for the image formation process is not correct due to spatially varying nominal tissue data values. This can occur for one of two reasons, either the tissue itself has physical properties that genuinely vary depending upon the location, or the values appear to change due to inhomogenaeity in the measurement system. The former of these we will return to below. The latter factor is exemplified by data acquired using surface coils (Figure 5(a) and (b)) and can be corrected if we can determine the spatially varying sensitivity (or gain) of the system, in the form of a multiplicative correction image. This is a very difficult thing to do reliably, particularly in the presence of partial volume effects. In general there is no substitute for trying to avoid the problem by using a well shimmed homogenous acquisition.

Of the algorithms described above the only one which could potentially deal with field inhomogenaeity without modification is the edge based approach, which operate in a purely local fashion. As we have already seen, this technique is restricted to data which has very good contrast to noise characteristics. Thus a technique for gain correction may still be necessary in some circumstances. There are two approaches to determining a gain correction. The first involves building a low parameter model for the expected gain correction into the solution for the label probabilities. These parameters can then be adjusted via an optimisation process which minimises the variances of the pure tissues [3]. This approach has several drawbacks. Firstly we may not know the correct parametric function for a given correction image, it would be very easy to assume a functional form which did not match the true characteristics. Secondly, the approach cannot work well if there are regions of unmodelled tissue in the data, so pathalogical data is once again excluded. Finally, determination of a set of parameters will need to be achieved via an iterative process if it is to stand any chance of making use of robust statistical assumptions. Iterative processes on data sets of this size are both slow and unreliable.

Calculation of a smooth correction image can be perfomed as follows;

- estimation of local image noise
- estimation of local image relative gradients $\Delta_x = (\partial I/\partial x)/I$, $\Delta_y = (\partial I/\partial y)/I$ and variances σ_x^2 σ_y^2.
- Maximum Likelihood estimation of smoothed local derivative using statistical averaging with a stability term for missing data w_{reg} (points with large gradient relative to noise) which assumes no image slope 0_{reg}.

$$\Delta_x^{ML}(x,y) \; = \; \frac{S \otimes (\Delta_x(x,y)/\sigma_x^2(x,y) + 0_{reg})}{S \otimes (1/\sigma_x^2(x,y) + w_{reg})}$$

- Integration of these derivatives along any path L from l_0 to $l \; = \; (x,y)$ can be witten as

$$\int_{l_0}^{l} \Delta_l^{ML}(l)dl \; = \; \int_{l_0}^{l} \frac{\partial F}{F_l} \; = \; [log(F_l)]_{l_0}^{l}$$

defining the starting point as unity gain gives the relative gain factor to that point $F(xy)$

$$F(x,y) \; = \; F_l \; = \; exp(\int_{l_0}^{l} \Delta_l^{ML}(l)dl)$$

The regularisation for missing data requires us to iterate the algorithm a few times for data with large regions of indeterminate slope.

Box 6: Gain correction using local slope.

The alternative approach involves assuming that the image is composed of homogenous regions of tissue separated by partial volume boundaries. Provided that we can detect partial volume regions (using for example a local contrast or derivative estimate), we can estimate the local relative gain change across a voxel in any uniform region. Applying the method to image slices from a 3D volume there will be two relative gain change images, one for the horizontal and the other for vertical changes. There will be some regions where we have no estimates, and some relative gain estimates will be more accurate than others depending upon the local signal to noise. However, spatial gain variations are expected to be locally smooth and we can make direct use of this information. By smoothing the local gain change by an amount less than the expected level of smoothness in the data we can fill in the missing data and increase the accuracy and stability of local estimates. This must be done using an appropriate statistical calculation which also takes account measurement accuracy. The relative horizontal and vertical gain changes determined can then be used to compute (via integration) an estimate of the original gain variation image. Typical results are shown in Figure 5 (c) and (d).

In comparison to the iterative parametric approach, this technique is simple, fast, reliable (non-iterative) and does not have to assume a particular parametric form for the gain variation [11]. Yet it can also deal with unmodelled data provided that it is composed of homogenous regions, or regions that have high spatial derivative (and therefore get excluded as image discontinuities). For large regions of slight inhomogenaiety there will be a distortion of the local estimated gain variation due ti the use of the regularisation term w_{reg}.

Like all analysis tasks, field inhomogenaety correction will only work reliably if the statistical charateristics of the data conforms to those assumed during algorithm design. Unfor-

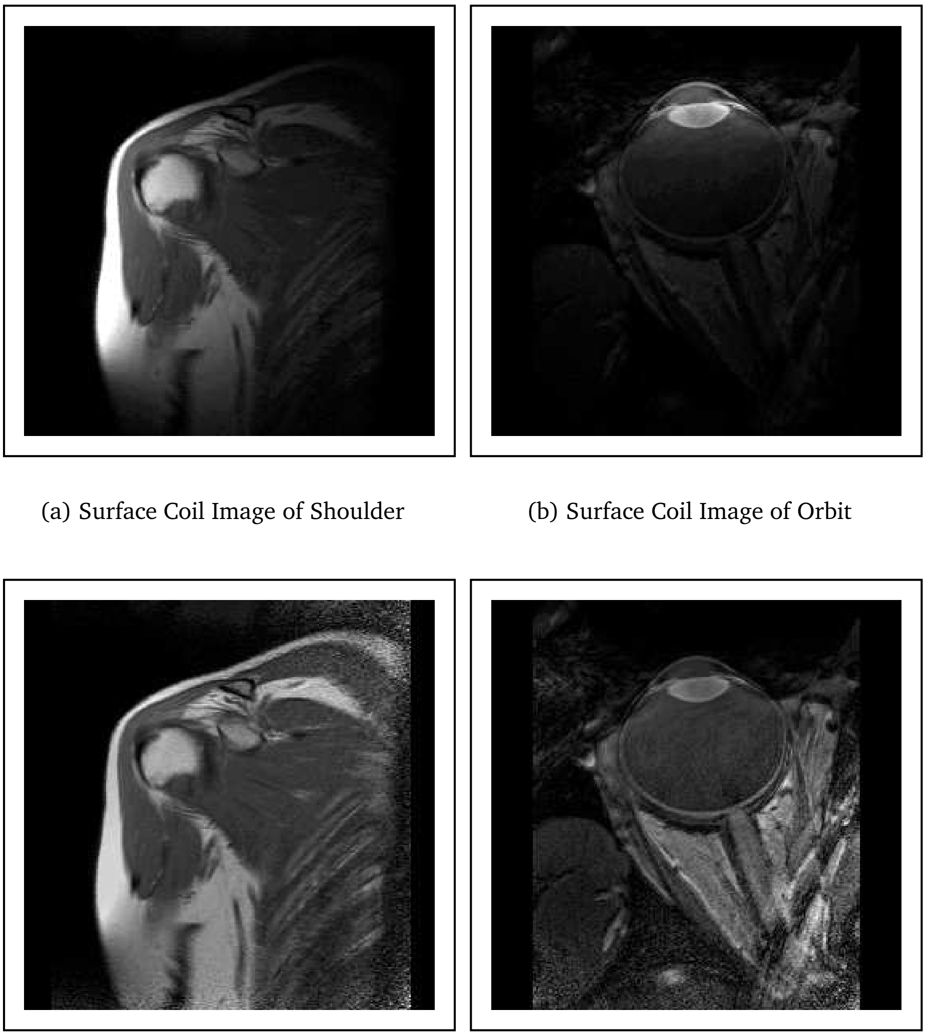

(a) Surface Coil Image of Shoulder

(b) Surface Coil Image of Orbit

(c) Corrected (a)

(d) Corrected (b)

Figure 5: Field Inhomogenaety Correction

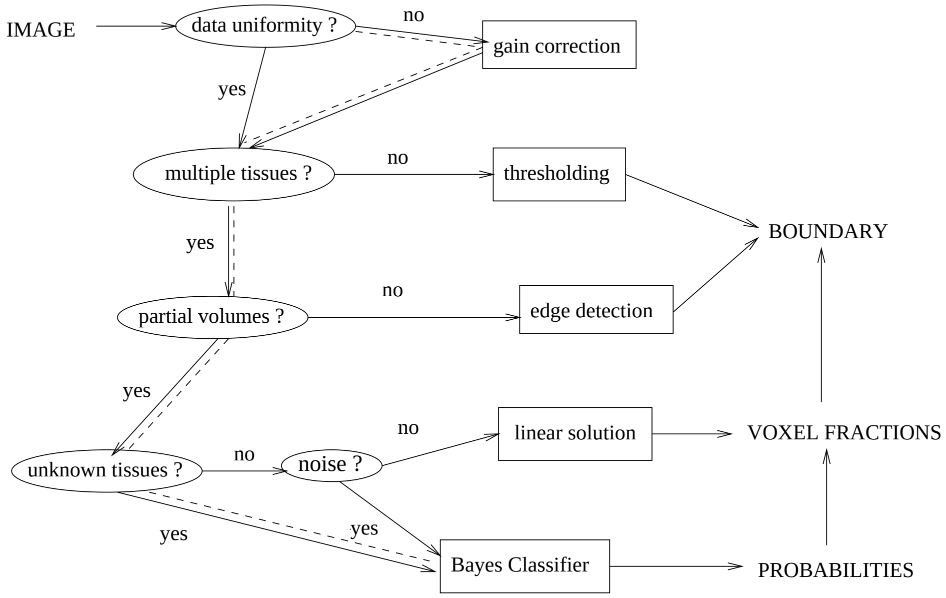

Figure 6: Tissue segmentation strategy.

tunately this is not an easy thing to determine automatically and there are inevitably some classes of images, either due to acquisition or anatomy, which cannot be corrected in this way. It is however, possible to perform a validation of the correction process by checking that the output data has been "improved" in some way. This can be done using measures based loosely upon concepts of information, though we do not believe that this approach is a valid way to design the correction process, we have addressed these issues in [19].

Conclusions

In this paper we have illustrated some of the common approaches to voxel based MR image segmentation and attempted to relate them with regard to the underlying assumptions used in their design. In particular we have done this through the observation that segmentation involves the need to identify the most likely cause for the observed image data, in terms of partial volume contributions. We have explained how this ultimately results in probabilistic approaches to volumetric estimation which break from the conventional idea of treating image segmentation as a labelling problem.

The overall strategy for selecting a segmentation method based upon the characteristics of the data is shown diagramatically in Figure 6. Answers to each of the questions in the bubbles determines the correct approach for a particular data set. One component of algorithm evaluation can therefore be done at the theoretical level of what variabilities we are taking account of in the model. The above diagram specifies the tests which need to be done in order to confirm that an algorithmic approach is at least appropriate. Clearly, formal evaluation is then also necessary for any subset of algoriths which may be identified as suitable in order to establish the "best".

The most general approach to tissue segmentation, which deals with all of the common problems found in typical data sets, is shown by the dotted curve and comprises gain correction and Bayes estimation of conditional probabilities. As this method can be implemented as a quick and reliable algorithm this is likely to be the preferred method for general image segmentation. However, by relating several approaches and explaining their assumptions regarding volumetric estimation, we hope to have conveyed the message that there is no single correct way of segmenting data which can be applied to every data set. In some cases relatively simple approaches are adequate, yet in others, even the more sophisticated approaches may not work. Thus although quantitative analysis of images has a lot to offer data interpretation it is still the case that much care is needed so that data sets are acquired in a way that they can be correctly processed. We have explained how field inhomogenaety is a particlular problem with quantitative analysis and suggested that the best way to deal with this is to avoid the problem using well shimmed acquisitions.

Another issue which we have touched upon is the amount of prior knowledge available for use use during prcessing. We have suggested caution regarding the idea of combining multiple sources of prior knowledge, due to the potential bias that this can cause in subsequent measurement. How much of the information from, edge boundaries, shape and expected location (atlas) can be legitimately combined for quantitative tasks is still an area of research in the image processing community.

All analysis techniques presented here are avaliable within the TINA freeware package distributed from our web site [22].

References

1. C.M.Bishop, Neural Networks for Pattern Recognition, Clarendon Press, Oxford, 66 ff, 1995.

2. P.A. Bromiley, M.L.J. Scott, M. Pokrić, A.J. Lacey and N.A. Thacker, Bayesian and Non-Bayesian Probabilistic Models for Magnetic Resonance Image Analysis, Image and Vision Computing, Special Edition; The use of Probabilistic Models in Computer Vision.21,10,251-264, 2003.

3. R. Guillemaud and J.M.Brady, Estimating the bias Field of MR Images, IEEE TRANS. on Medical Imaging, 16(3), 238-251, 1997.

4. S.Webb, The Physics of Medical Imaging, Medical Science Series, Pub. Adam Hilger ,Bristol, Philadelphia and New York, 1988.

5. W.E.Lorensen, H.E.Cline, Marching Cubes: A High Resolution 3D Surface Construction Algorithm, SIGGRAPH '87, ACM Computer Graphics, 21(4), 163-169, 1987.

6. Canny, J.F., 'A Computation Approach to Edge Detection', IEEE PAMI, 8, pp. 679-698, 1986.

7. W.H.Press B.P.Flannery S.A.Teukolsky W.T.Vetterling, Numerical Recipes in C, Cambridge University Press 1988.

8. W.M.Wells, E.L.Grimson, R.Kikinis et al. Adaptive segmentation of MRI data. IEEE Trans. on Medical Imaging, 15(4), 429-442, 1996.

9. N.A.Thacker, A.Jackson, X.P.Zhu and K.L.Li, 'Accuracy of Tissue Volume Estimation in MR Images ', Proc. MIUA , 137-140, Leeds, 1998 .

10. K.Fukenaga, 'Introduction to Statistical Pattern Recognition', 2ed, Academic Press, San Diego (1990).

11. E.Vokurka, N.Thacker, A.Jackson, "A Fast Model Independant Method for Automatic Correction of Correction of Intensity Non-Uniformity in MRI Data." JMRI, 10, 4, 550-562, 1999.

12. E.A.Vokurka., A. Herwadkar, N.A.Thacker, R.T.Ramsden and A.Jackson,. Using Bayesian Tissue Classification to Improve the Accuracy of Vestibular Schwannoma Volume and Growth Measurement. AJNR, 23, 459-467, 2002.

13. Laidlaw DH, Fleischer KW, Barr AH, Partial-volume bayesian classification of material mixtures in MR volume data using voxel histograms, IEEE Trans. Med. Imag., vol. 17, no. 1, 74-86, Feb. 1998.

14. I. POOLE, *Optimal Probabilistic Relaxation Labeling*, Proc. BMVC 1990, BMVA, 1990.

15. M. Pokric, N.A. Thacker, M.L.J.Scott and A.Jackson, Multi-Dimesional Medical Image Segmentation with Partial Voluming, MIUA, Birmingham, 77-80, 2001.

16. M.Pokric, N.A.Thacker, M.L.J.Scott and A.Jackson, The Importance of Partial Voluming in Multi-dimensional Medical Image Segnmentation, Proc. MICCAI 2001, 1293-1294, 2001.

17. B.D.Ripley, Appendix A in Pattern Recognition and Neural Networks, Cambridge University Press, 1996.

18. H.Rusinek, et. al. Alzheimer's Disease: measuring loss of cerebral grey matter with MR imaging. Radiology, 178(1), p109-14, 1991.

19. N.A.Thacker, A.J.Lacey and P.A.Bromiley, Validating MRI Field Homogenaeity Correction Using Information Measures., BMVC 2002, pp626-635, Cardiff, 2002.

20. D.C.Williamson, N.A.Thacker, S.R. Williams and M.Pokric, Partial Volume Tissue Segmentaion using Grey Level Gradient. Proc. MIUA 2002, Portsmouth, 17-20, 2002.

21. L. Xu and M.I.Jordan, On Convergence Properties of the E.M. Algorithm for Gaussian Mixtures, A.I. Memo No. 1520 C.B.C.L. Paper no 111, 1995.

22. URL: www.niac.man.ac.uk